Variable-temperature inelastic light scattering spectroscopy of nickel oxide: Disentangling phonons and magnons

M. M. Lacerda, F. Kargar, E. Aytan, R. Samnakay, B. Debnath, J. X. Li, A. Khitun, R. K. Lake, J. Shi, and A. A. Balandin

Citation: Appl. Phys. Lett. **110**, 202406 (2017); doi: 10.1063/1.4983810
View online: http://dx.doi.org/10.1063/1.4983810
View Table of Contents: http://aip.scitation.org/toc/apl/110/20
Published by the American Institute of Physics

Variable-temperature inelastic light scattering spectroscopy of nickel oxide: Disentangling phonons and magnons

M. M. Lacerda,[1,2] F. Kargar,[1,3] E. Aytan,[1,3] R. Samnakay,[1,3] B. Debnath,[4] J. X. Li,[5] A. Khitun,[3,6] R. K. Lake,[4,6] J. Shi,[5,6] and A. A. Balandin[1,6,a)]

[1]*Nano-Device Laboratory (NDL) and Phonon Optimized Engineered Materials (POEM) Center, Department of Electrical and Computer Engineering, University of California – Riverside, Riverside, California 92521, USA*

[2]*Campus Duque de Caxias, Universidade Federal do Rio de Janeiro, Rio de Janeiro 25245-390, Brazil*

[3]*Materials Science and Engineering Program, Bourns College of Engineering, University of California – Riverside, Riverside, California 92521, USA*

[4]*Laboratory for Terascale and Terahertz Electronics (LATTE), Department of Electrical and Computer Engineering, University of California – Riverside, Riverside, California 92521, USA*

[5]*Department of Physics and Astronomy, University of California – Riverside, Riverside, California 92521, USA*

[6]*Spins and Heat in Nanoscale Electronic Systems (SHINES) Center, University of California – Riverside, Riverside, California 92521, USA*

(Received 13 February 2017; accepted 7 May 2017; published online 19 May 2017)

We report the results of an investigation of the temperature dependence of the magnon and phonon frequencies in NiO. A combination of Brillouin-Mandelstam and Raman spectroscopies allowed us to elucidate the evolution of the phonon and magnon spectral signatures from the Brillouin zone center (GHz range) to the second-order peaks from the zone boundary (THz range). The temperature-dependent behavior of the magnon and phonon bands in the NiO spectrum indicates the presence of antiferromagnetic (AF) order fluctuation or a persistent AF state at temperatures substantially above the Néel temperature (T_N=523 K). Tuning the intensity of the excitation laser provides a method for disentangling the features of magnons from acoustic phonons in AF materials without the application of a magnetic field. Our results are useful for the interpretation of the inelastic-light scattering spectrum of NiO and add to the knowledge of its magnon properties important for THz spintronic devices. *Published by AIP Publishing.*
[http://dx.doi.org/10.1063/1.4983810]

Nickel oxide (NiO) has been extensively studied in the past for a variety of applications in catalysts, gas sensors, electrochemical films, battery electrodes, and photo-devices.[1–6] Recently, NiO has attracted a renewed, and fast growing, interest as an antiferromagnetic (AF) electrically insulating material for applications in spintronic devices, particularly those operating at THz frequencies.[7] NiO has also been used for spin current enhancement as an intermediate nanometer-scale layer in magnetic material—NiO—heavy metal heterostructures.[8,9] In general, the utilization of spin currents instead of electric currents has the advantage of reducing Joule heating. The latter constitutes a promising approach for the next generation of devices for low-power-dissipation information processing.[10,11] Further development of spintronics requires better understanding of the physics of magnons and phonons and their interactions in AF materials.

Despite a number of previous studies of the Raman spectrum of NiO,[12–17] there is substantial discrepancy among the reported values for the phonon and magnon frequencies and between the theory and the experiment.[18–21] Usually, it is difficult to distinguish magnon peaks from phonon peaks, particularly when they appear as a broad band, which is a combination of both.[22,23] The application of a magnetic field—a conventional approach for identification of magnons—is difficult for NiO due to the large field strength required for inducing measurable magnon peak shifts. It has been reported[24] that the application of a magnetic field with the intensity $B = 7$ T to NiO resulted in the Raman magnon frequency change of less than $\sim 3\,cm^{-1}$. The magnetic ordering affects phonon energies via spin–phonon and spin–lattice coupling.[24,25] Calculations of the phonon band structure, which do not include the effects of spin ordering, predict phonon energies that differ from the experiments.[19,26] Similarly, magnon dispersion, calculated from the Heisenberg model for spins located on the same and adjacent crystalline planes without the inclusion of the spin-lattice interactions, leads to discrepancy with experimental data. For example, the most studied two-magnon (2M) peak in the Raman spectrum of NiO, which is observed at $\sim 1500\,cm^{-1}$ at room temperature (RT), has been theoretically predicted[17,27] in the range of $1800\,cm^{-1}$–$1900\,cm^{-1}$. The difficulties in the interpretation of the inelastic-light scattering spectra of NiO are not limited to the optical phonon frequencies ($\sim 100\,cm^{-1}$–$2000\,cm^{-1}$) measured by Raman spectroscopy. They are also present in the acoustic phonon frequency range (2 GHz–900 GHz; 1 THz = $33.37\,cm^{-1}$) measured by Brillouin–Mandelstam spectroscopy (BMS).[28,29] The low signal-to-noise ratios for BMS peaks of magnons from the Brillouin zone (BZ) center coupled with the overlap in their frequency with phonons and discrepancy with the theoretical predictions further complicate the peak assignment.

a)Author to whom correspondence should be addressed: balandin@ee.ucr.edu

In this letter, we report the results of a combined Raman and BMS study of NiO crystals over a wide temperature range. Raman spectra were measured using the cold-hot cell with the temperature changing from RT to 873 K. Unlike previous Raman studies of NiO,[12–17] we focus on the temperatures above T_N. The temperature increase during BMS experiments was achieved by increasing the excitation laser intensity to 250 mW on the sample surface, which resulted in local temperatures exceeding 700 K. Based on the results of BMS studies, we propose a simple method for distinguishing BZ-center (Γ point) magnon peaks from acoustic phonon peaks using the excitation-laser power dependence of the magnon peak intensity. We have also established that the intensity of the BZ-edge two-magnon peak in the Raman spectrum of NiO is strongly suppressed above the Néel temperature where the crystal undergoes reconstruction from the AF to the paramagnetic state.[12,22] However, the 2M peak does not disappear completely at $T \sim 600$ K (above T_N=523 K), indicating AF order fluctuations or persistent AF ordering. Our results constitute the first proof of AF order above T_N by inelastic spectroscopy (both Raman and BMS). Raman studies of NiO reported in Refs. 13–17 were limited to $T < 500$ K.

The single crystal nature of bulk NiO (111) samples selected for this study has been confirmed by X-ray diffraction (XRD) measurements. NiO has an A-type AF crystalline structure consisting of ferromagnetically (FM) aligned (111) planes that are AF aligned with respect to each other.[18,28,29] Below the Néel temperature, the AF ordering is accompanied by a slight rhombohedral distortion.[29] The Raman measurements were performed in the backscattering configuration under a laser excitation of $\lambda = 488$ nm (2.54 eV). All measurements were performed with the samples placed inside a cold-hot cell under an argon atmosphere to ensure that no oxidation occurred at elevated temperatures. The excitation power was kept at 2 mW to avoid local heating. Under such conditions, the temperature of the sample is the same as set by the cold-hot cell. Raman spectra were accumulated during both the heating and cooling cycles. For the accurate measurement of the characteristic magnon and phonon frequencies, all Raman spectra were fitted with Voigt functions.

Figures 1(a) and 1(b) illustrate the evolution of the Raman spectrum of (111) NiO during the heating and cooling cycles, respectively. The fact that the spectral changes are completely reversible when the samples are heated up to ~600 K and cooled back to RT proves that the Raman spectral changes are due to the intrinsic phonon and magnon properties of NiO, and they are not related to any surface oxidation or contamination. The Raman bands measured at RT are in agreement with previous studies of bulk NiO single crystals.[13] One can recognize the transverse optical (TO) phonon mode at ~403 cm^{-1} and the longitudinal optical (LO) phonon mode at ~520 cm^{-1}. The two-phonon excitations observed at ~720 cm^{-1}, 899 cm^{-1}, and 1100 cm^{-1} correspond to 2TO, TO + LO, and 2LO modes, respectively. The pronounced two-magnon peak has the frequency of 1500 cm^{-1}. The 2M peak originates from two counter-propagating magnons with the wave vectors from the opposite edges of BZ allowed by the momentum conservation.[30] The 2M band is Raman active due to an induced non-zero

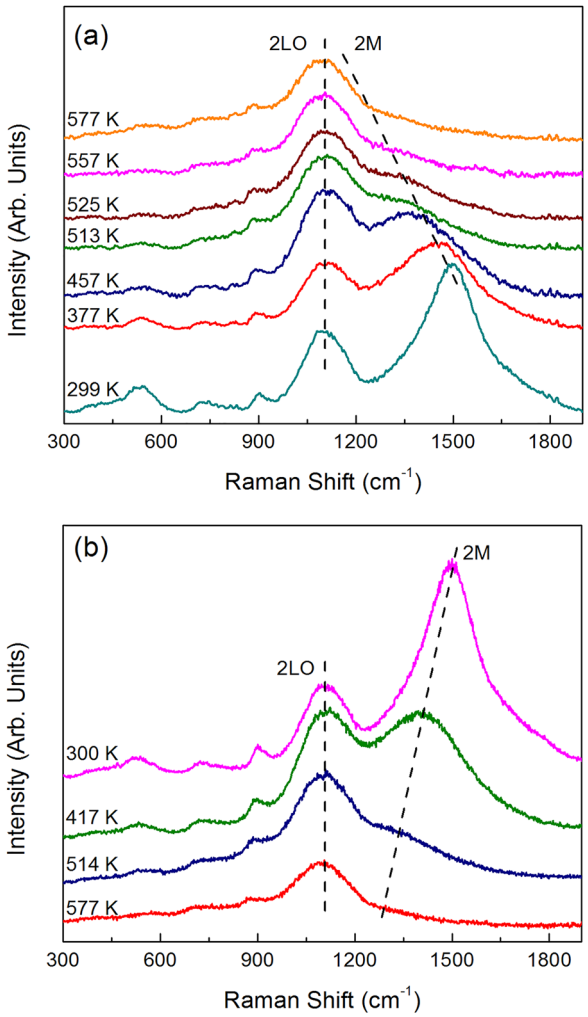

FIG. 1. Evolution of the Raman spectrum of NiO at different temperatures during the heating (a) and cooling (b) cycles. The changes in the Raman spectrum are fully reversible within this temperature range. Note traces of the two-magnon peak (2 M) at T = 577, which is substantially above Néel temperature $T_N = 523$ K.

net dipole momentum at X and Z symmetry points in the BZ.[31] Its energy approximately corresponds to twice the magnon energy at the BZ boundary.[18,32]

One can see substantial changes in the Raman spectrum of NiO as the temperature increases and crosses the Néel temperature. Near $T_N = 523$ K, the characteristic 2M band broadens, shifts to lower frequencies, and decreases in intensity. The main observation is that 2M signatures are persistent at temperatures substantially above T_N.[31] Similar features have been observed in other AF materials such as $RbMnF_3$ (Ref. 33), MnF_2, and $KNiF_3$ (Ref. 34). The nature of the AF phase transition in NiO, i.e., first-order *vs.* second-order, has been debated.[34–36] Several theoretical studies suggested the first-order transition.[36–39] The experimental evidence that the AF phase transition in NiO is continuous (i.e., the second order) is limited to one neutron diffraction study.[34] A more recent report of neutron diffraction measurements for NiO[40] discussed the problems associated with this technique in determining the structural and magnetic transitions and suggested that rhombohedral distortion of the lattice of NiO was ignored in the previous study.[34] Our Raman data with clear signatures of the magnon band above the Néel temperature constitute an

independent proof of AF ordering above T_N using a different experimental technique. Another observation from Fig. 1 is that the temperature dependence of the 2LO phonon band is much weaker than that of the 2M band. The 2LO phonon frequency remains near 1100 cm^{-1} in the examined temperature range.

As the next step in our study, we increased the temperature substantially above T_N to T = 873 K. At temperatures above ~800 K, the Raman spectrum of NiO loses reversibility [Fig. 2(a)]. At T = 617 K and T = 673 K, the LO, LO + TO, and 2LO phonon modes are still measurable and their spectral positions are consistent with the data presented in Fig. 1. However, in addition to these modes, two new peaks at ~1345 cm^{-1} and 1580 cm^{-1} emerge. The first-order phonon modes are not expected in the paramagnetic state of NiO (above T_N) unless there are parity-breaking imperfections in the sample or a persistent AF state above T_N. The presence of the 2LO band and traces of TO and LO peaks above T_N are other indicators of residual AF ordering, in line with our observations for the 2 M band. From T = 673 K up to T = 873 K, we observe the decreasing intensity of the 2LO phonon band and increasing intensity of new peaks at 1345 cm^{-1} and 1580 cm^{-1}. The Raman spectral changes above T ~ 800 K are irreversible, i.e., the RT spectrum is not restored upon cooling down the sample. XRD analysis confirms that the NiO sample undergoes structural changes and becomes polycrystalline [see Fig. 2(b)]. The transition to polycrystalline NiO or the loss of O can explain the appearance of new peaks in the Raman spectrum measured significantly above T_N.

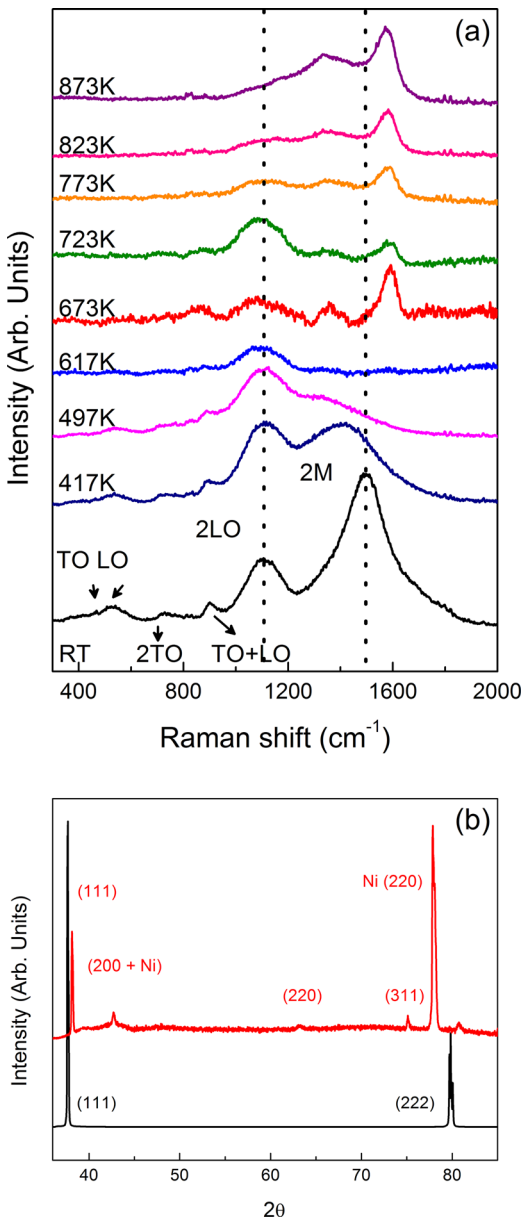

FIG. 2. (a) Raman spectrum of NiO over an extended temperature range reaching T = 873 K. The changes in the Raman spectrum of NiO heated above 600 K are irreversible. Note the appearance of new peaks at T = 617 K. (b) XRD spectrum of NiO before (black curve) and after (red curve) heating to T = 873 K. The changes in the XRD spectrum are in line with Raman data and confirm the structural changes in NiO. The XRD data are taken at RT.

We now analyze the temperature effects on magnons and acoustic phonons near the Γ point in the BZ. BMS experiments were carried out in backscattering geometry using a solid-state diode pumped laser operating at λ=532 nm. The laser light was focused on the samples through a lens with $NA = 1.4$. The scattered light was collected with the same lens and directed to the high-resolution six-pass tandem Fabry-Perot interferometer. During the experiment, the laser light was focused on the sample at a fixed incident angle of 20° with respect to the normal to the sample's surface. The probing phonon and magnon wave-vector in this experiment is $q_B = 4\pi n/\lambda$, where n is the refractive index of NiO at the laser excitation wavelength [$n \sim 2.4$–2.5 (Ref. 37)]. Assuming $n \sim 2.4$, the probing wave-vector for bulk phonons and magnons is 56.7 μm^{-1}. The laser power on the sample surface was varied from ~60 mW to ~250 mW. Changing the laser power, one can effectively control the local temperature of the sample.

In Fig. 3(a), we present the BMS spectrum of NiO with two prominent peaks at 37.9 GHz (1.26 cm^{-1}) and 65.3 GHz (2.18 cm^{-1}), which correspond to the transverse acoustic (TA) and longitudinal acoustic (LA) phonon branches, respectively. A broad shoulder close to the TA phonon frequency is considered to be a "zero-frequency" magnon band in some studies.[27,41] However, clear experimental evidence for the nature of this band is still missing. Figure 3(b) shows the BMS spectra in a larger free spectrum range under different incident laser powers. At a laser power of 58 mW (black curve), there is a broad peak at ~356 GHz (11.88 cm^{-1}), which has been assigned as the zone-center magnon.[41] This is the only magnon band, which was clearly observed in our BMS experiments. This band has been reported in other studies as well, although there is an uncertainty in its frequency.[41,42] It should be noted that the number and spectral positions of the zone-center magnons in NiO have been the subjects of debates.[15,17,18,20,23,27,41] For example, Ref. 23 based its description of the spin structure and dynamics in NiO on the assumption of existence of a magnon peak around 0.9 cm^{-1} although cannot be resolved in the noisy spectral background. The most prominent zone-center magnon is usually observed at ~1 THz.[15,17,27,42] The changes in the magnon peak position with temperature further complicate the peak assignment.

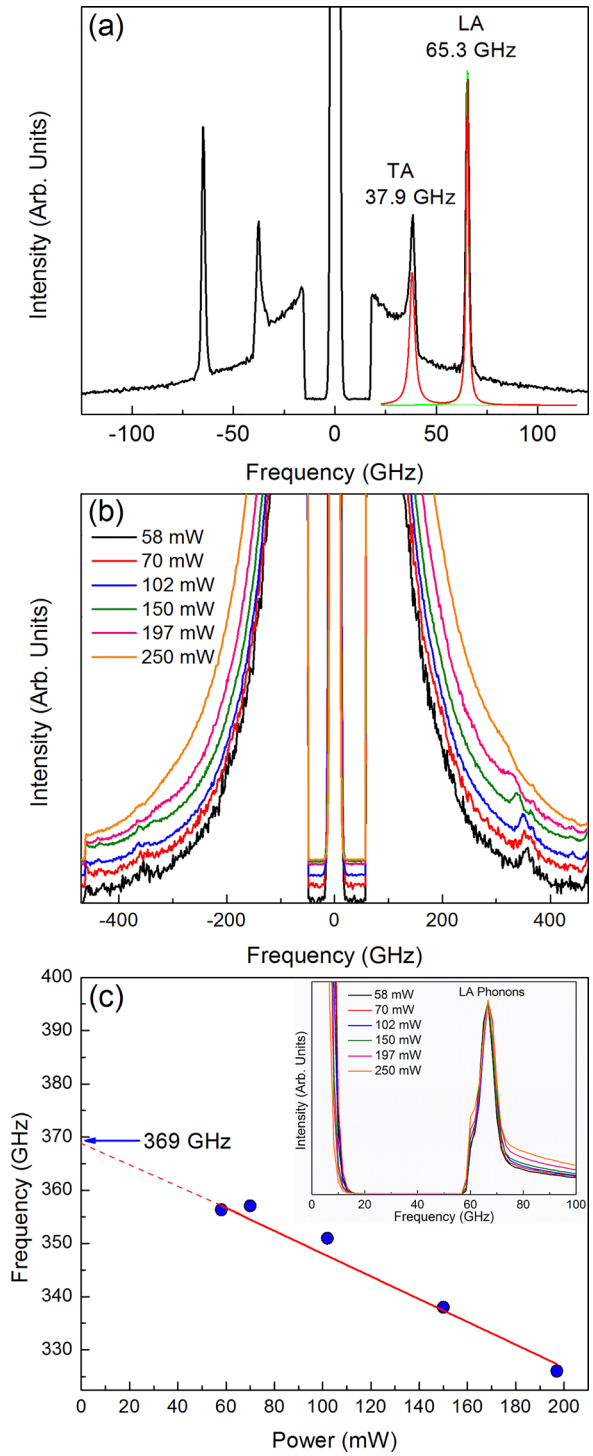

FIG. 3. (a) BMS spectrum of NiO with pronounced TA and LA phonon peaks. (b) BMS spectrum of NiO at different excitation laser powers on a sample surface. The one-magnon peak at ∼356 GHz shifts to lower frequency and disappears completely as the temperature increases above T_N owing to the laser heating. (c) The change in the magnon peak position with the laser power. The intensity of the one-magnon peak is normalized with respect to the intensity of the LA phonon peak at ∼65 GHz for each laser power. The inset shows the LA phonon peak as a function of laser power. The results demonstrate that the magnon signatures can be conveniently identified from their laser power dependence without the use of the magnetic field or cold-hot cells.

Using the peak at ∼356 GHz as an example, we now demonstrate a convenient method for distinguishing magnon signatures, which can be readily used in BMS experiments even without cold-hot cells for external temperature control.

Figure 3(b) shows the evolution of the peak with the laser power, P, increasing from 58 mW to 250 mW, which results in the corresponding increase in the local temperature. The intensity of the ∼356 GHz peak has been normalized to the intensity of the LA phonon peak at ∼65 GHz. The position of the LA phonon does not change with increasing power, which indicates that the change in the refractive index, n, in this temperature range is negligible (the probing wave-vector in a BMS experiment is a linear function of n). At the same time, with increasing laser power, the frequency and the intensity of the ∼356 GHz peak decrease, and finally, at $P = 250$ mW, the peak disappears completely. The frequency of this peak versus P is plotted in Fig. 3(c). We argue that the peak disappearance confirms its magnon origin, and it is due to the local temperature increase above T_N as the laser power on the sample reaches high values. The LA phonon peak hardly changes its frequency and intensity with P, and it remains prominent at this high excitation power level [see the inset of Fig. 3(c)]. Heating the sample with the excitation laser above T_N provides a convenient method for the assignment of the magnon peaks in NiO and other AF materials without the use of the magnetic field and cold-hot cell.

To verify the fact that temperature above T_N is achieved in this experiment, we simulated heat diffusion in a NiO crystal using the finite-element method implemented with COMSOL. The laser heat source was modeled as

$$Q_{LASER} = \eta P_{LASER} e^{\left(-\frac{x^2+y^2}{\sigma^2}\right)} \alpha e^{-\alpha|z|}, \quad (1)$$

where P_{LASER} is the incident laser power, $\eta = 0.7$ is the emissivity of the NiO surface, and α is the absorption coefficient. The laser source has a Gaussian distribution in space, characterized by the standard deviation $\sigma = R/3$, where $R = 15\ \mu$m is the laser spot radius. The factor $\alpha e^{-\alpha|z|}$ in Eq. (1) governs the propagation of the incident light intensity, I, according to the Beer-Lambert law $\partial I/\partial z = -\alpha I$. The absorption coefficient, α, depends on both the local temperature and the laser wavelength. We have used the linear extrapolation of the values of α reported in Ref. 43. The temperature variation inside the sample is governed by the conventional heat transfer equation. Figure 4 shows the maximum temperature of the hotspot and the minimum temperature inside the sample at different incident laser powers. One can see that as the applied laser power increases to ∼130 mW, the hotspot temperature reaches the Néel temperature, although the overall sample temperature remains below T_N. At ∼250 mW, the temperature of the whole sample increases beyond the Néel temperature. The temperature distribution profile in the sample is shown in the inset of Fig. 4. The distribution near the hot spot area (red color) depends on the Gaussian profile of the laser power and the exponential decay of the light intensity inside NiO (z axis). The sample temperature reaches the steady-state within ∼1 min, which is much smaller than actual heating time in the experiment.

In summary, the zone-boundary magnon bands and zone-center TO and LO phonons have been analyzed over a wide temperature range extending beyond 870 K. The Raman and BMS spectra indicate that spin correlations resulting in persistent AF ordering or AF order fluctuations

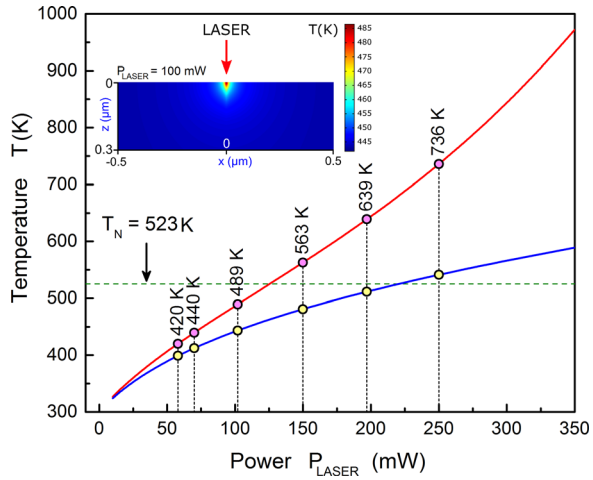

FIG. 4. Calculated temperature as a function of the excitation laser power for a given NiO sample. The Néel temperature T_N is shown as the horizontal line. The red curve corresponds to the highest temperature in the hot spot, while the blue curve corresponds to the lowest temperature on the back of the sample. The inset presents temperature distribution in the simulated NiO sample. The laser power is set as 100 mW. The calculations support the conclusion that $T > T_N$ is achieved in the BMS experiments with variable laser power.

exist well above the Néel temperature. An elegant method for disentangling the features of magnons from acoustic phonons in the BMS spectrum without the application of a magnetic field is also demonstrated. This is an important capability considering that very high magnetic fields ($B \sim 7$ T) are required for inducing measurable shifts to magnon peaks in the NiO spectrum.

The work at UC Riverside was supported in part by the Spins and Heat in Nanoscale Electronic Systems (SHINES), an Energy Frontier Research Center funded by the U.S. Department of Energy, Office of Science, Basic Energy Sciences (BES) under Award No. SC0012670. M.M.L. also acknowledges Conselho Nacional de Desenvolvimento a Pesquisa (CNPq) and the program Ciencias sem Fronteiras for financial support during her research at UC Riverside.

[1]M. Gong, W. Zhou, M.-C. Tsai, J. Zhou, M. Guan, M.-C. Lin, B. Zhang, Y. Hu, D.-Y. Wang, J. Yang, S. J. Pennycook, B.-J. Hwang, and H. Dai, Nat. Commun. **5**, 4695 (2014).
[2]Y. Ichiyanagi, N. Wakabayashi, J. Yamazaki, S. Yamada, Y. Kimishima, E. Komatsu, and H. Tajima, Phys. B: Condens. Matter **329**, 862 (2003).
[3]I. Hotovy, J. Huran, L. Spiess, S. Hascik, and V. Rehacek, Sens. Actuators, B **57**, 147 (1999).
[4]T. Fukui, S. Ohara, H. Okawa, T. Hotta, and M. Naito, J. Power Sources **86**, 340 (2000).
[5]J. Wang, L. Wei, L. Zhang, C. Jiang, E. Siu-Wai Kong, and Y. Zhang, J. Mater. Chem. **22**, 8327 (2012).
[6]V. Biju and M. Abdul Khadar, Spectrochim. Acta, Part A **59**, 121 (2003).
[7]T. Kampfrath, A. Sell, G. Klatt, A. Pashkin, S. Mährlein, T. Dekorsy, M. Wolf, M. Fiebig, A. Leitenstorfer, and R. Huber, Nat. Photonics **5**, 31 (2011).
[8]H. Wang, C. Du, P. C. Hammel, and F. Yang, Phys. Rev. Lett. **113**, 97202 (2014).
[9]W. Lin, K. Chen, S. Zhang, and C. L. Chien, Phys. Rev. Lett. **116**, 186601 (2016).
[10]J. Nishitani, K. Kozuki, T. Nagashima, and M. Hangyo, Appl. Phys. Lett. **96**, 221906 (2010).
[11]R. A. Patil, C.-W. Su, C.-J. Chuang, C.-C. Lai, Y. Liou, Y.-R. Ma, X. Shen, A. Perumal, Y.-R. Ma, I.-K. Yoo, D. H. Seo, X.-S. Li, J.-B. Park, J.-H. Lee, and Y. Park, Nanoscale **8**, 12970 (2016).
[12]R. E. E. Dietz, G. I. I. Parisot, and A. E. E. Meixner, Phys. Rev. B **4**, 2302 (1971).
[13]R. E. E. Dietz, W. F. Brinkman, A. E. Meixner, and H. J. Guggenheim, Phys. Rev. Lett. **27**, 814 (1971).
[14]M. J. Massey, N. H. Chen, J. W. Allen, and R. Merlin, Phys. Rev. B **42**, 8776 (1990).
[15]D. J. Lockwood, M. G. Cottam, and J. H. Baskey, J. Magn. Magn. Mater. **104**, 1053 (1992).
[16]M. Pressl, M. Mayer, P. Knoll, S. Lo, U. Hohenester, and E. Holzinger-Schweiger, J. Raman Spectrosc. **27**, 343 (1996).
[17]M. Grimsditch, L. E. McNeil, and D. J. Lockwood, Phys. Rev. B **58**, 14462 (1998).
[18]M. T. Hutchings and E. J. Samuelsen, Phys. Rev. B **6**, 3447 (1972).
[19]R. A. Coy, C. W. Tompson, and E. Gürmen, Solid State Commun. **18**, 845 (1976).
[20]A. P. Cracknell and S. J. Joshua, in *Mathematical Proceedings of the Cambridge Philosophical Society* (1969), pp. 493–504.
[21]A. C. Gandhi, C.-Y. Huang, C. C. Yang, T. S. Chan, C.-L. Cheng, Y.-R. Ma, and S. Y. Wu, Nanoscale Res. Lett. **6**, 485 (2011).
[22]N. Mironova-Ulmane, A. Kuzmin, I. Steins, J. Grabis, I. Sildos, and M. Pärs, J. Phys. Conf. Ser. **93**, 12039 (2007).
[23]J. Milano and M. Grimsditch, Phys. Rev. B **81**, 94415 (2010).
[24]D. J. Lockwood and M. G. Cottam, J. Appl. Phys. **64**, 5876 (1988).
[25]P. K. Pandey, R. J. Choudhary, D. K. Mishra, V. G. Sathe, and D. M. Phase, Appl. Phys. Lett. **102**, 142401 (2013).
[26]A. C. Gandhi, J. Pant, S. D. Pandit, S. K. Dalimbkar, T.-S. Chan, C.-L. Cheng, Y.-R. Ma, and S. Y. Wu, J. Phys. Chem. C **117**, 18666 (2013).
[27]M. Grimsditch, S. Kumar, and R. S. Goldman, J. Magn. Magn. Mater. **129**, 327 (1994).
[28]H. Kondoh and T. Takeda, J. Phys. Soc. Jpn. **19**, 2041 (1964).
[29]W. L. Roth, Phys. Rev. **110**, 1333 (1958).
[30]M. G. Cottam, J. Phys. C: Solid State Phys. **5**, 1461 (1972).
[31]M. G. Cottam and D. J. Lockwood, *Light Scattering in Magnetic Solids* (Wiley-Interscience, 1986).
[32]T. Fujiwara, W. Gebhardt, K. Petanides, and Y. Tanabe, J. Phys. Soc. Jpn. **33**, 39 (1972).
[33]P. A. Fleury, W. Hayes, and H. J. Guggenheim, J. Phys. C: Solid State Phys. **8**, 2183 (1975).
[34]T. Chatterji, G. J. McIntyre, and P.-A. Lindgard, Phys. Rev. B **79**, 172403 (2009).
[35]D. Mukamel and S. Krinsky, Phys. Rev. B **13**, 5065 (1976).
[36]K. Binder and D. P. Landau, Phys. Rev. B **30**, 1477 (1984).
[37]R. J. Powell and W. E. Spicer, Phys. Rev. B **2**, 2182 (1970).
[38]H. T. Diep and H. Kawamura, Phys. Rev. B **40**, 7019 (1989).
[39]M. T. Heinilä and A. S. Oja, Phys. Rev. B **48**, 16514 (1993).
[40]A. M. Balagurov, I. A. Bobrikov, S. V. Sumnikov, V. Y. Yushankhai, and N. Mironova-Ulmane, JETP Lett. **104**, 88 (2016).
[41]J. Milano, L. B. Steren, and M. Grimsditch, Phys. Rev. Lett. **93**, 77601 (2004).
[42]M. Takahara, H. Jinn, S. Wakabayashi, T. Moriyasu, and T. Kohmoto, Phys. Rev. B **86**, 94301 (2012).
[43]R. Newman and R. M. Chrenko, Phys. Rev. **114**, 1507 (1959).